RESEARCH ARTICLE

The Relationship between Cranial Structure, Biomechanical Performance and Ecological Diversity in Varanoid Lizards

Matthew R. McCurry[1,2,3]*, Michael Mahony[2], Phillip D. Clausen[4], Michelle R. Quayle[1], Christopher W. Walmsley[1], Tim S. Jessop[5], Stephen Wroe[4,6], Heather Richards[4], Colin R. McHenry[1,4]

1 Department of Anatomy and Developmental Biology, Monash University, Melbourne, Australia, 2 School of Environmental and Life Science, University of Newcastle, Newcastle, Australia, 3 Geosciences, Museum Victoria, Melbourne, Australia, 4 School of Engineering, University of Newcastle, Newcastle, Australia, 5 Department of Zoology, University of Melbourne, Melbourne, Australia, 6 The Function, Evolution & Anatomy Research Lab, Zoology Division, School of Environmental and Rural Sciences, University of New England, Armidale, Australia

* m.r.mccurry1@gmail.com

Abstract

Skull structure is intimately associated with feeding ability in vertebrates, both in terms of specific performance measures and general ecological characteristics. This study quantitatively assessed variation in the shape of the cranium and mandible in varanoid lizards, and its relationship to structural performance (von Mises strain) and interspecific differences in feeding ecology. Geometric morphometric and linear morphometric analyses were used to evaluate morphological differences, and finite element analysis was used to quantify variation in structural performance (strain during simulated biting, shaking and pulling). This data was then integrated with ecological classes compiled from relevant scientific literature on each species in order to establish structure-function relationships. Finite element modelling results showed that variation in cranial morphology resulted in large differences in the magnitudes and locations of strain in biting, shaking and pulling load cases. Gracile species such as *Varanus salvadorii* displayed high strain levels during shaking, especially in the areas between the orbits. All models exhibit less strain during pull back loading compared to shake loading, even though a larger force was applied (pull =30N, shake = 20N). Relationships were identified between the morphology, performance, and ecology. Species that did not feed on hard prey clustered in the gracile region of cranial morphospace and exhibited significantly higher levels of strain during biting (P = 0.0106). Species that fed on large prey clustered in the elongate area of mandible morphospace. This relationship differs from those that have been identified in other taxonomic groups such as crocodiles and mammals. This difference may be due to a combination of the open 'space-frame' structure of the varanoid lizard skull, and the 'pull back' behaviour that some species use for processing large prey.

Introduction

The varanoid lizards comprise three modern genera (*Varanus*, *Heloderma* and *Lanthanotus*) and make up important components of various modern predator guilds [1,2]. For example, the monsoonal tropics of Northern Australia contain up to 11 sympatric varanoid species [2] that function as apex predators, mesopredators, insectivores and scavengers [2,3]. Despite having a conserved body plan, varanoids exhibit considerable variation in body size [4,5], limb dimensions [6] and skull structure [7]. Whilst the influence of varanid (referring to the genus *Varanus*) body size on locomotion and ecology has been explored, the consequences and contribution of skull variation for biomechanical and ecological performance have received less attention [5,8,9]. Here we quantify variation in cranial morphology between a number of extant varanoid species and examine the biomechanical and ecological consequences of these differences.

Varanoid lizards were previously considered a monophyletic group [10] however some recent phylogenetic analyses group *Varanus* and *Lanthanotus* together with *Shinisaurus* in Paleoanguimorpha, and find *Heloderma* to be a member of a sister group (the Neoanguimorpha) to these [11]. Within a phylogenetic context, the inclusion of *Heloderma* represents an outgroup to the other specimens included in the study (which are all part of the Paleoanguimorpha). Recent revisions of squamate relationships indicate that the phylogeny may still not be completely resolved [12,13]. Here we use the term varanoid to refer to *Varanus*, *Lanthanotus* and *Heloderma* as a useful ecological or functional grouping, but note that future consensus of phylogenetic analyses may find it to be polyphyletic.

Varanoid lizards exhibit a range of behaviours during capture and processing of prey. Prey is predominantly killed using a bite. If too large to be swallowed whole, prey must be processed into manageable pieces for consumption. To do this varanoid species can shake prey from side to side to tear off chunks [14], or use a sawing pull-back movement where the teeth are drawn back through the item [15,16]. From a biomechanical perspective, a major role of the skull is to transmit the force generated by jaw and postcranial musculature to the prey whilst resisting the loads induced by these behaviours.

Identifying mechanistic links between form and function is challenging because the complex morphology of biological structures, as well as often complex interplay between morphology and performance, makes analytical approaches difficult [17]. Simulation based techniques, such as finite element analysis (FEA), provide a valuable methodology to investigate the effect of complex differences in cranial structure on performance measures [18]. When combined with modern morphometric analyses, these structural models represent a powerful method for predicting the influence of morphology on mechanical performance [19,20,21,22,23]. Palaeontologists and biologists have gained great insights by utilizing FEA to explore how variations in morphology influence structural performance [21,23,24,25,26,27,28,29,30,31,32,33,34,35]. These studies have greatly increased understanding of how (and to what degree) biological form relates to the structural performance (ability to resist loading) of the skull and the influence this has on the animal's ecology.

The cranial design of varanoid lizards is highly fenestrated compared to mammalian and crocodilian skulls [36]. In engineering design a highly fenestrated structure is termed a "space frame" in contrast to a "shell" construction. In the context of cranial mechanics, it is not clear whether space frame structures exhibit the same form-function relationships as shell constructions. Logically the strength of space frame constructions will be dictated to a high degree by the thickness, position and orientation of the struts, whereas in shell constructions it will be determined by the thickness of the continuous wall that is used to distribute loads. Presumably space-frame skulls are expected to work in a different manner to shell structured skulls with

load being transferred through the struts perpendicular to its long axis. The mechanics of shell-type skulls have been investigated a number of times using finite element analysis [24,26,31,32,33,34,37,38,39,40,41,42,43,44]; space-frame skulls have not been examined to the same degree, with only single specimen studies [45,46,47,48,49].

Here we present a comparative cranial FEA of varanoid species, with the aim of quantitatively assessing the relationship between the shape of varanoid lizard crania and mandibles, their structural performance to biologically relevant loading (biting, shaking and pulling forces) and the dietary ecology of the species. Our study includes high resolution models of 13 skulls, making it one of the largest three dimensional finite element analyses of cranial mechanics performed to date.

Beam theory provides a means of calculating the load carrying characteristics of a simple beam structure [50]. Based on beam theory we predicted that:

1. Lower strain levels will occur in taller craniums and mandibles during bite loading.

2. Lower strain levels will occur in wider craniums and mandibles during shake loading.

3. Lower strain levels will occur in taller and wider craniums and mandibles during pull loading.

    When comparing performance and ecology it is predicted that:

1. Species that feed on hard prey items will exhibit less strain during bite loading than other species.

2. Species that feed on large prey items will exhibit less strain during shake and pull loading than other species.

Methods

Data acquisition and morphometric analysis

Computer tomography (CT) scans of 13 varanoid skulls, representing 12 species, were obtained from online libraries (www.digimorph.org) or through scanning (at either Newcastle Mater Hospital using a Toshiba Aquilion 64 slice CT or at Sydney University using an Xradia MicroXCT-400 micro CT). The specimens were selected from the approximately 79 possible varanoid species to maximise phylogenetic and morphological variation (Fig 1). These specimens are housed in a number of repositories (Table 1). Two of the specimens (*V. gouldii* and *V. komodoensis*) represent sub-adult specimens. Mimics V13 (MATERIALISE, Belgium) was used to convert scan data into three dimensional surface geometry of the cranium and mandible. Morphometrics were undertaken using both 3D and linear methods. Thirteen linear measurements were taken in the 3D CAD software package Rhino [51] (Fig 2). LANDMARK [52] was used to select the location in 3D space of a series of 24 landmarks and 11 curves on the cranium and 14 landmarks and 22 curves on the mandible for geometric morphometric analysis (Fig 2). These locations were exported as.pts files, manually reformatted, and then imported into MOPHOLOGIKA [53] where Procrustes superimposition and principle component analysis were undertaken (S1 File).

Finite element analysis

High resolution versions of the geometries used in the morphometric analysis were converted into solid meshes composed of simple tetrahedral elements (tet4s), here termed bricks, using Harpoon (http://www.sharc.co.uk). Each surface.stl file was imported before being meshed
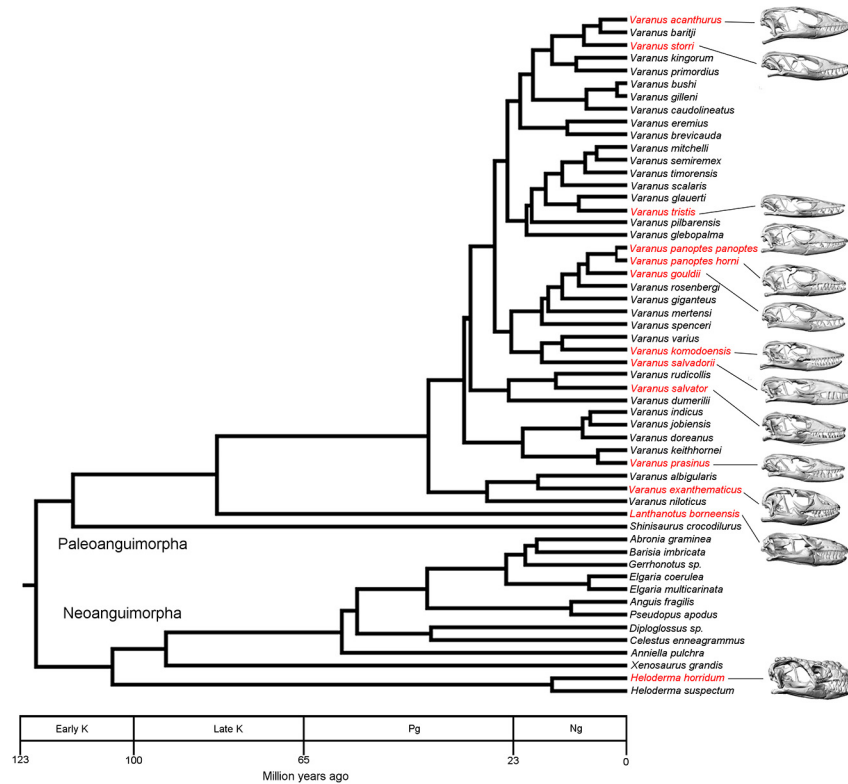
Fig 1. Phylogenetic sampling. Phylogeny of Paleoanguimorpha and Neoanguimorpha showing the taxa used within this study in red text. Labels on timescale: K, Cretaceous; Pg, Paleogene; Ng, Neogene. Adapted from Vidal [11]. Note that the lateral views of the skulls are not to scale.

doi:10.1371/journal.pone.0130625.g001

firstly using the "wrapping" function and secondly the "all tet" function. The wrapping function allowed for surface and internal geometry to be standardised between models through adjusting the surface cell size and with it the degree of captured geometry. Only major internal geometry such as the mandibular cavity was included. The solid mesh of each cranium consisted of 1 million bricks (±4%). The mandible was then meshed so that the tetrahedral bricks were approximately equal in size to those of the cranium (±1%). These solid models were imported into Strand 7 V2.4.4 (www.strand7.com) for FEA. Isotropic homogeneous material properties (Young's Modulus = 22.8 GPa, density = 1050 kg/m^3) were used for bone in all models based on published data of a *Varanus exanthematicus* femur [54]. Homogeneous material properties were chosen over heterogeneous material properties because of: 1) a general lack of data on varanoid bone properties and 2) to better isolate biological shape as a variable within the analysis. A hinge system was implemented to allow the mandible to pivot in relation to the cranium [27] and the gape angle was set to 10 degrees. The jaw hinge was created by extruding beams in the x axis from the lateral side of the bottom of the quadrate. These beams were then subdivided into two equal parts. The end furthest from the skull was released in rotation in the x axis to allow for the jaw to pivot in relation to the cranium. Rigid links were then created to take the place of the half of the beam closest to the skull and to join the freed end to the mandible. A user defined cylindrical co-ordinate system was created around the jaw hinge axis for use in defining the loads (applied forces) and freedoms (used to constrain the model) of each load case.

Table 1. Specimens used in this study.

Taxon	Specimen number	Repository of original specimen	Source of digital data	Dorsal cranial length (cm)
Heloderma horridum	TNHC 64380	Texas Memorial Museum	Digimorph online library	5.7
Lanthanotus borneensis	YPM 6057	Yale Peabody Museum of Natural History	Digimorph online library	1.8
Varanus acanthurus	UTA 13015	The Amphibian and Reptile Diversity Research Centre at the University of Texas at Arlington	Digimorph online library	2.7
Varanus exanthematicus	FMNH 58288	Florida Museum of Natural History	Digimorph online library	4.9
Varanus gouldii	AMR 142826	The Australian Museum	Digimorph online library	4.0
Varanus komodoensis	AMR 106933	The Australian Museum	Sydney University	11.2
Varanus panoptes panoptes	AMR 75084	The Australian Museum	Newcastle Mater Hospital	7.4
Varanus panoptes horni	TMM-M-1295	Texas Memorial Museum	Newcastle Mater Hospital CT	5.3
Varanus prasinus	AMR 166380	The Australian Museum	Sydney University	3.2
Varanus salvadorii	QMJ 14498	Queensland Museum	Newcastle Mater Hospital	11.2
Varanus salvator	FMNH 35144	Florida Museum of Natural History	Digimorph online library	11.9
Varanus storri	AMR 143912	The Australian Museum	Sydney University	2.2
Varanus tristis	AMR 143919	The Australian Museum	Sydney University	3.1

doi:10.1371/journal.pone.0130625.t001

Muscles were simulated by attaching 120 truss elements between muscle attachment locations based on the diagrams presented in Holliday [55]. The number of truss elements used to represent each muscle was calculated based on the bone surface areas of the various muscles on *Varanus panoptes horni* (the species of median volume). Muscle elements were defined as either being part of the temporal or pterygoid muscle groups which resulted in 56 temporal truss elements and 64 pterygoid truss elements. Each truss element was assigned a diameter of 1.944423 cm and applied with a tensile force based on the cross sectional area of the two major muscle groups outlined in Walmsley et al.[21] and McHenry [56]. The numbers of beams used to represent each muscle were selected based on the relative surface area of the muscle attachment areas in *Varanus panoptes panoptes*. Table 2 displays which muscles were classified into each of these groups as well as the number of beams used to represent the muscle. Muscle elements were evenly distributed over the attachment areas. The same force was applied to each truss within its respective muscle group (temporal or pterygoid). Data on the forces calculated for the muscles can be found in S1 Table. In whole, this method of model construction assumes that the muscle attachment sites of the various species are identical whilst including differences in the relative size of the two muscle groups. Load cases were used to simulate the forces generated by relevant feeding behaviours. Each model was scaled to the same volume as *V. panoptes horni*, following the methods used in Walmsley et al.[21,57]; applied forces were not scaled. The three load cases simulated were:

1. **Bite loading,** where pretension was applied through muscle beams. The occipital condyle was restrained in all 6 degrees of freedom and the four largest teeth in the middle of the tooth row were restrained in circumferential translation centred on the jaw hinge axis. The right upper and lower teeth were also restrained in medial-lateral translation. The magnitude of force applied through each muscle beam (constructed as a "truss" element in
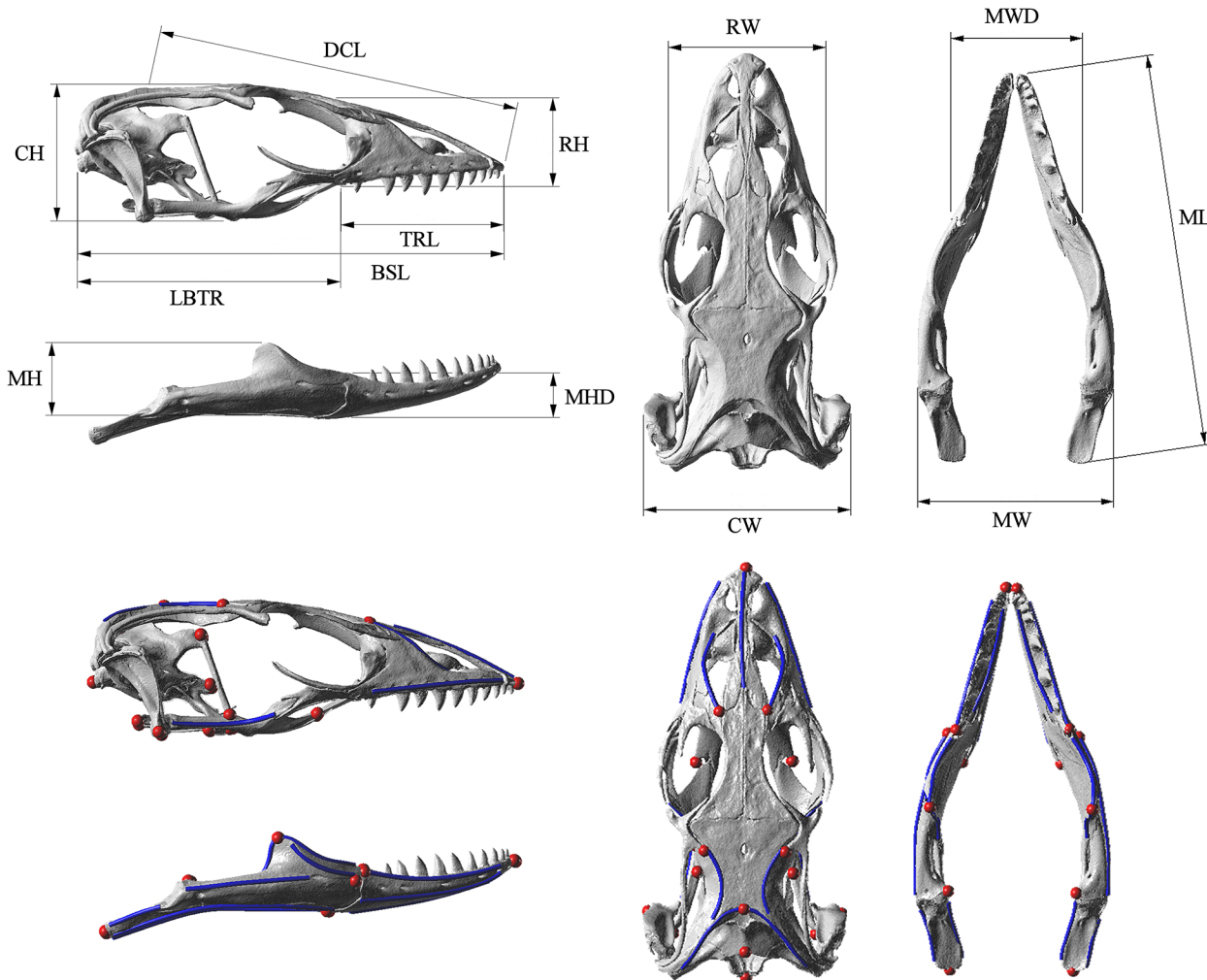
Fig 2. Linear measurements and landmarks used in morphometric analysis. Morphometric information used in this study. Top: linear measurements taken from specimens. Bottom: Points and curves used in geometric morphometric analysis. Point landmarks are shown in red and curves are shown in blue. Abbreviations and definitions for linear measurements can be found in S1 File. The specimen shown is *Varanus acanthurus*: UTA 13015.

doi:10.1371/journal.pone.0130625.g002

Strand7) was standardised as to generate the same node reaction forces at the teeth (i.e. the same resultant bite force) of 47.8 N (Predicted bite force for the *Varanus panoptes horni*

Table 2. Functional classification of jaw muscles into two muscle groups (temporalis and pterygoid).

Individual muscle	Abbreviation	Muscle group	Number of elements
m. pterygoideus	mPT	Pterygoid	34
m. levator pterygoideus	mLPt	Pterygoid	4
m. protractor pterygoideus	mPPt	Pterygoid	26
m. adductor mandibulae posterior	mAMP	Temporalis	6
m. adductor mandibulae externus superficialis	mAMES	Temporalis	16
m. adductor mandibulae externus medialis	mAMEM	Temporalis	10
m. pseudotemporalis superficialis	mPSTs	Temporalis	16
m. pseudotemporalis profundus	mPSTp	Temporalis	2
m. adductor mandibulae externus profundus	mAMEP	Temporalis	6

doi:10.1371/journal.pone.0130625.t002

1. Bite 2. Shake 3. Pull
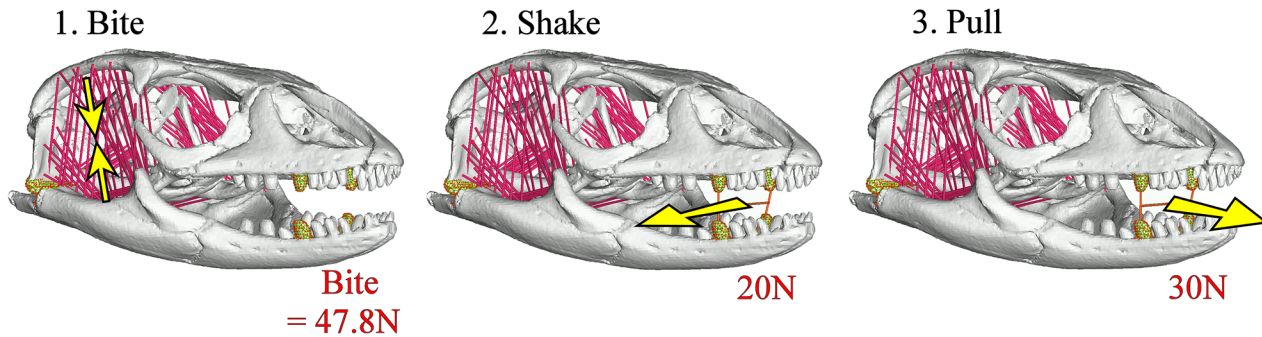

Bite
= 47.8N

20N

30N

Fig 3. Load cases. The three load cases undertaken in this study: 1. Biting where the models are constructed to bite with the same resultant force of 47.8 N; 2. Shaking where a force of 20N is applied laterally to the middle teeth and 3. Pulling where a force of 30N is applied anteriorly to the middle teeth. Note that within the Shake and Pull load cases muscles do not apply force but brace the skull. The model also shows muscle beams that were used to apply loads in biting (pink), H beams (orange) that were used to apply load to the teeth during shake and pull load cases and surface beams (green) that distribute load across the restrained teeth, jaw hinge surface and occipital condyle. The specimen shown is *Varanus exanthematicus*: FMNH 58288.

model)(Fig 3). The muscle beam forces applied to each model to give that standardised resultant bite force are shown in S1 Table.

2. **Shake loading**, where a force of 20N was applied in a lateral direction using a system of beams connecting the four middle teeth. Muscle beams were set with a Young's Modulus of 15 MPa with no pretension applied to simulate the muscles bracing the skull [21,56]. The occipital condyle was restrained in all 6 degrees of freedom and the centre of the beams connecting the middle teeth was restrained in an arc around the jaw hinge axis (Fig 3).

3. **Pull back loading,** where a force of 30N was applied in an anterior direction using a system of beams connecting the four middle teeth. Muscle beams were again set with a Young's Modulus of 15 with no pretension applied to simulate the muscles bracing the skull. The occipital condyle was restrained in all 6 degrees of freedom and the centre of the beams connecting the middle teeth was restrained in an arc around the jaw hinge axis (Fig 3).

A series of beams were also used to reinforce areas where artificial (high) strain was expected. These areas include the restrained teeth, the occipital condyle (also a site of restraint), the jaw hinge surfaces and small areas around the site of each muscle beam attachment.

Ecological classifications

Data on the diet of species was compiled from relevant scientific literature [58,59,60,61,62,63, 64,65,66,67,68,69,70,71,72]. Because of the nature of much of the published data, we were only able to draw broad categories based on the presence or absence of prey items with certain characteristics (Tables 3 and 4). The two categories were: 1) whether the diet of the species included prey items considered as hard, or harder, than a bird egg (e.g. crabs) and 2) whether the diet of the species included prey items larger than could be swallowed whole (e.g. large mammals such as wallabies).

Statistical analysis

The resulting strains for each brick, in either the cranium or the mandible, during each load case were exported to and analysed in R [73]. R was then used to identify the 95% von Mises (VM) strain values of each case following the methods of Walmsley et al. [21,73]; this 95% von Mises strain constitutes the largest elemental (individual brick) value of strain in the model if the highest 5% of all elemental values are removed. The R code has been uploaded as a

Table 3. Ecological classifications.

Species	Hard Prey	Large Prey
Heloderma horridum	Y	N
Lanthanotus bornensis	Y	N
Varanus acanthurus	Y	N
Varanus exanthematicus	Y	N
Varanus gouldii	N	Y
Varanus komodoensis	Y	Y
Varanus panoptes horni	Y	Y
Varanus panoptes panoptes	Y	Y
Varanus prasinus	N	Y
Varanus salvadorii	Y	Y
Varanus salvator	Y	Y
Varanus storri	N	N
Varanus tristis	N	N

doi:10.1371/journal.pone.0130625.t003

supplementary file (S2 File) as well as instructions on its use (S3 File). Examination of resulting strain values using mean, 25%, 50%, 75%, 90%, 95% and 98 values all showed similar patterns in results between models. Patterns between models using 99, 99.9 and maximum values did however vary slightly to the others indicating that localised peaks may be affecting these values (Fig 4). The 95% value presumably represents a way to compare the performance of the models whilst ignoring peak loading artefacts.

Tests for phylogenetic signal in the morphometric results (using the phylogeny presented in Vidal [11]) were undertaken using a permutation test with 10000 randomisation rounds in MorphoJ. Partial least squares analysis (PLS) was undertaken in JMP V11 to test the relationship between morphology and the strain levels resulting from FEA load cases. Only one latent variable was included in each comparison because the addition of extra variables did not greatly improve the percentage of variation explained. Variable importance values and percentage variation values were also calculated in JMP. In the case of linear variables, the analysis was run between each single performance measure (VM strain during biting, shaking and pulling) and all morphological variables of the mandible or cranium, the percentage variation explained is only presented for the best correlated morphological variable. We also tested for intraspecific allometry using the same PLS method, comparing centroid size and PC1 and PC2 of the cranium and mandible. Multivariate analysis of variance (MANOVA), with a repeated measures response specification, was undertaken in JMP V 11 to test the relationship between ecological variables and performance. Univariate tests (ANOVA) were then used to test each individual combination of variable after the initial analysis.

Results

Ecological classification

All species are opportunistic predators, feeding on a range of vertebrate and invertebrate prey including small lizards, small and large mammals, bird and lizard eggs, amphibians, worms, beetles, centipedes, spiders, crabs, fish and birds. However, noticeable variation in diet is also reported in the published literature [58,59,60,61,62,63,64,65,66,67,68,69,70,71,72]. This variation appears to reflect both habitat and capabilities in prey capture (Tables 3 and 4). No species solely feed on invertebrates, however *V. acanthurus* and *V. storri* were found to prey on insects along with small prey such as lizards. Other notable specialisation included *H. horridum*,

Table 4. Diet of the study species.

Food item	H.hor	L.bor	V.exa	V.slt	V.pra	V.sdi	V.kom	V.gou	V.pan	V.stor	V.aca	V.tri
worms		1										
other insects	1		1	1	1	1	1	1	1	1	1	1
beetles	1		1		1		1	1	1		1	1
orthopterans			1		1			1	1	1	1	1
centipedes			1						1		1	
spiders					1			1	1	1	1	
scorpions			1									
snails			3								3	
mussels									3			
crabs		3		3								
fish		1		2								
small lizards			1			1		1	1	1	1	1
large lizards						1		1	1			
snakes									1			
lizard eggs	1			1				1	1	1		1
amphibians			1	1					1			
birds	1		1	1		1						1
bird eggs	3		3	3		3	3		3			
small mammals				1	2		1		1			
large mammals						2	2					
carrion				2		2		2	2			

1 = normal prey item

2 = food items too large to be eaten whole

3 = hard prey items. Data was compiled from relevant scientific literature. Note that dietary record for several species were incomplete.

which preys primarily on eggs and juvenile birds, and *V. komodoensis* and *V. salvadorii*, the only species within this analysis to feed on large mammals (Tables 3 and 4).

Morphometrics. Qualitatively, species of varanoid lizards differ substantially in cranial and mandibular morphology (Fig 5). Linear measurements taken on volume scaled models are shown in Table 5. Geometric morphometric analysis provided a more comprehensive picture of morphological variation. Within the cranium, Principal Component (PC) 1 and PC2 together only explained 58.26% of the differences in shape. PC1 was composed of differences in the height, width, length and curvature of the rostrum as well as the width of the skull roof. PC2 was represented by the height of the back of the skull and the area of the skull roof (Fig 6). Within the mandible, PC1 and PC2 together explained 65.07% of the variation in shape. PC1 was composed of differences in the overall width and height of the mandible as well as the position and height of the coronoid process. PC2 represented changes in the height of the coronoid process and comparative length of the tooth row (Fig 7).

Both phylogenetic and functional patterns are present within the results; a permutation test using a time calibrated phylogeny produced a P value of 0.0402 in the cranium and a P value of 0.0018 in the mandible indicating that the dataset contains significant phylogenetic influence [74]. *Heloderma horridum*, *Lanthanotus borneensis* and *Varanus exanthematicus* clustered in each of the PC plots, the Australian dwarf monitors (subgenus *Odatria*; included here are *V. acanthurus*, *V. storri*, and *V. tristis*) also clustered, occupying the top of the mandible morphospace. The test for interspecific allometry using PLS identified one pair of singular warp vectors
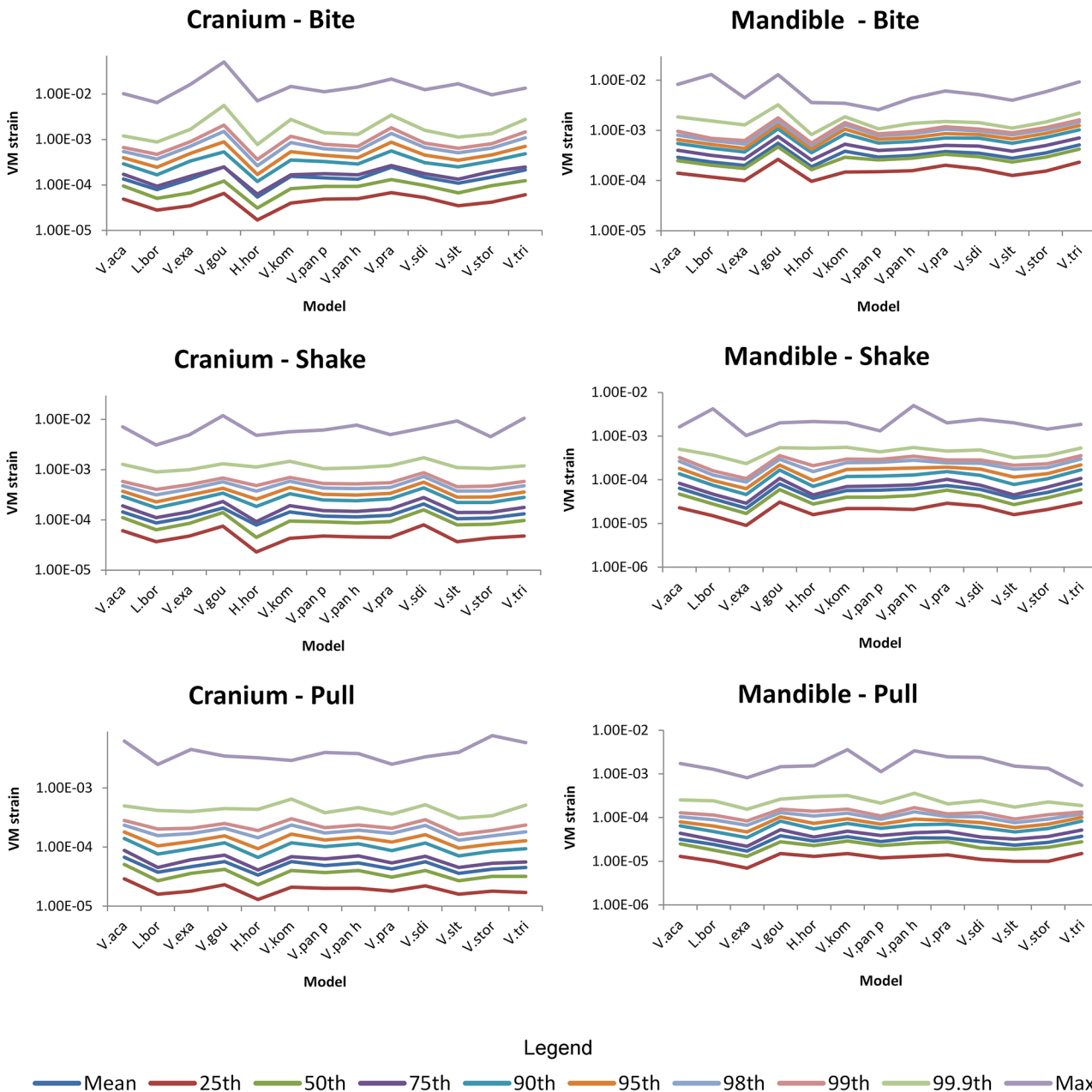
Fig 4. Comparison of possible summary values used as performance measures. Comparison of the pattern between models using various summary values. These were generated from von Mises strain values for each brick within the models. Note that all values, apart from the maximum, 99th and 99.9th values, depict a similar pattern in the results.

that were poorly correlated (Total variation explained for Y effects = 13.467), indicating that allometric trends in shape are small. The species that fed on prey larger than can be swallowed whole clustered in the centre left of the cranial morphospace and in the bottom left of the mandible morphospace. This morphospace is associated with thin and shallow mandibles and thin, long crania with comparatively long tooth rows. The species that feed on large prey items occupied a larger area of morphospace in the mandible analysis than in the cranial analysis (Figs 6 and 7).
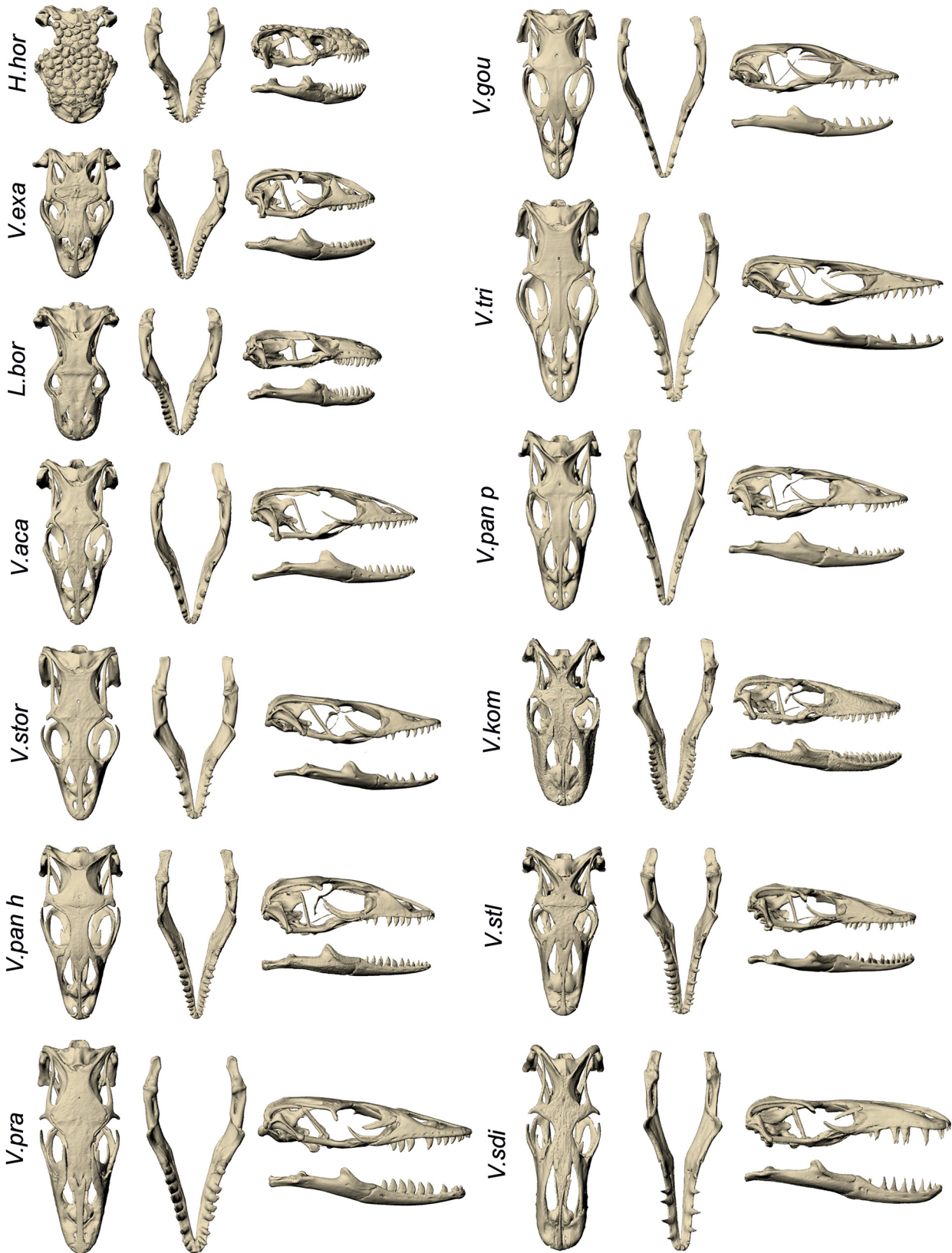
Fig 5. Visual comparison of cranial and mandibular morphology between specimens. The morphology of each specimen is shown in dorsal and lateral view for both the cranium and mandible. Species are ordered by cranial PC1 values. Abbreviations: H.hor, *Heloderma horridum;* L.bor, *Lanthanotus borneensis;* V.aca, *Varanus acanthurus;* V.exa, *Varanus exanthematicus;* V.gou, *Varanus gouldii;* V.kom, *Varanus komodoensis;* V.pan h, *Varanus panoptes horni;* V.pan p, *Varanus panoptes panoptes;* V.pra, *Varanus prasinus;* V.sdi, *Varanus salvadorii;* V.slt, *Varanus salvator;* V.stor, *Varanus storri;* V.tri, *Varanus tristis*.

Finite element analysis

Finite element modelling results showed that variation in cranial morphology resulted in large differences in the magnitudes and locations of strain in each load case (Figs 8–11). During bite loading, strain occurred in high levels within the pterygoid, epipterygoid, sides and front of the rostrum as well as in the mandible anterior to the jaw hinge axis (Fig 8). Low magnitudes of strain were observed in the crania of *H. horridum*, *L. borneensis and V. salvator* and the mandibles of *H. horridum*, *L. borneensis*, and *V. exanthematicus* in this load case.

There was considerably less strain associated with the mandible in shake loading compared to bite loading (Fig 11). Patterns of strain are similar in each model during shaking with high levels in the anterior of the mandible and across parts of the cranium, specifically in-between the orbits, the posterior part of the pterygoid bone, the epipterygoid, and the opisthotic and in localised areas close to the teeth at which forces were applied (Fig 9). The magnitude of strain within these areas varied considerably between species (Figs 8, 9 and 10). Gracile species such as *V. salvadorii* displayed high strain levels during shaking, especially in the areas between the orbits. *V. salvadorii* displayed strain values substantially higher than the other models. The *V. salvadorii*, *V. komodoensis* and *V. gouldii* models exhibited high VM strain values within the cranium. Considerably less variation in strain was observed in mandibles as opposed to the crania during this load case (Fig 11).

The areas of high strain during pull back loading include the pterygoid, epipterygoid and opisthotic bones as well as the sides of the rostrum and areas surrounding the teeth where forces were applied (Fig 10). All models exhibit less strain during pull back loading compared to shake loading, even though a larger force was applied (pull = 30N, shake = 20N). During pull back load cases strain values varied between each model. Within the cranium the highest observed strain values were in *V. acanthurus* followed by *V. komodoensis*, *V. salvadorii* and *V. gouldii*. Within the mandible strain magnitudes were high in the *V.gouldii* and *V.tristis* models

Table 5. Linear measurements (cm) from volume scaled models.

| Species	BSL	DCL	CH	CW	RH	RW	TRL	IOD	ML	MH	MW	MHD	MWD
Heloderma horridum	4.11	3.97	3.77	3.06	2.69	3.57	3.11	3.17	4.11	2.58	3.73	2.38	3.20
Lanthanotus bornensis	4.30	4.02	3.83	3.03	2.47	3.49	3.27	2.77	4.22	2.55	3.78	2.37	3.41
Varanus acanthurus	4.53	4.37	3.83	3.40	2.90	3.54	3.54	2.18	4.50	2.72	3.80	2.28	3.41
Varanus exanthematicus	4.20	4.02	3.80	3.19	2.90	3.46	3.37	2.27	4.22	2.73	3.78	2.11	3.38
Varanus gouldii	4.55	4.40	3.81	3.32	2.93	3.51	3.72	2.14	4.51	2.72	3.91	2.24	3.51
Varanus komodoensis	4.39	4.26	3.65	3.17	2.79	3.55	3.62	2.37	4.48	2.57	3.71	2.33	3.23
Varanus panoptes horni	4.45	4.30	3.68	3.37	2.94	3.45	3.61	2.13	4.45	2.66	3.68	2.10	3.30
Varanus panoptes panoptes	4.50	4.35	3.59	3.31	2.91	3.44	3.73	2.25	4.51	2.76	3.75	2.35	3.32
Varanus prasinus	4.52	4.35	3.53	3.17	2.81	3.41	3.73	2.37	4.45	2.46	3.74	2.08	3.40
Varanus salvadorii	4.55	4.39	3.54	3.15	2.75	3.30	3.78	2.10	4.52	2.46	3.59	2.22	3.01
Varanus salvator	4.38	4.23	3.71	3.15	2.72	3.33	3.60	2.31	4.41	2.64	3.69	2.41	3.24
Varanus storri	4.50	4.34	3.71	3.11	2.79	3.47	3.49	2.12	4.45	2.54	3.76	2.11	3.28
Varanus tristis	4.63	4.46	3.73	3.12	2.79	3.50	3.73	2.11	4.59	2.26	3.84	1.89	3.20
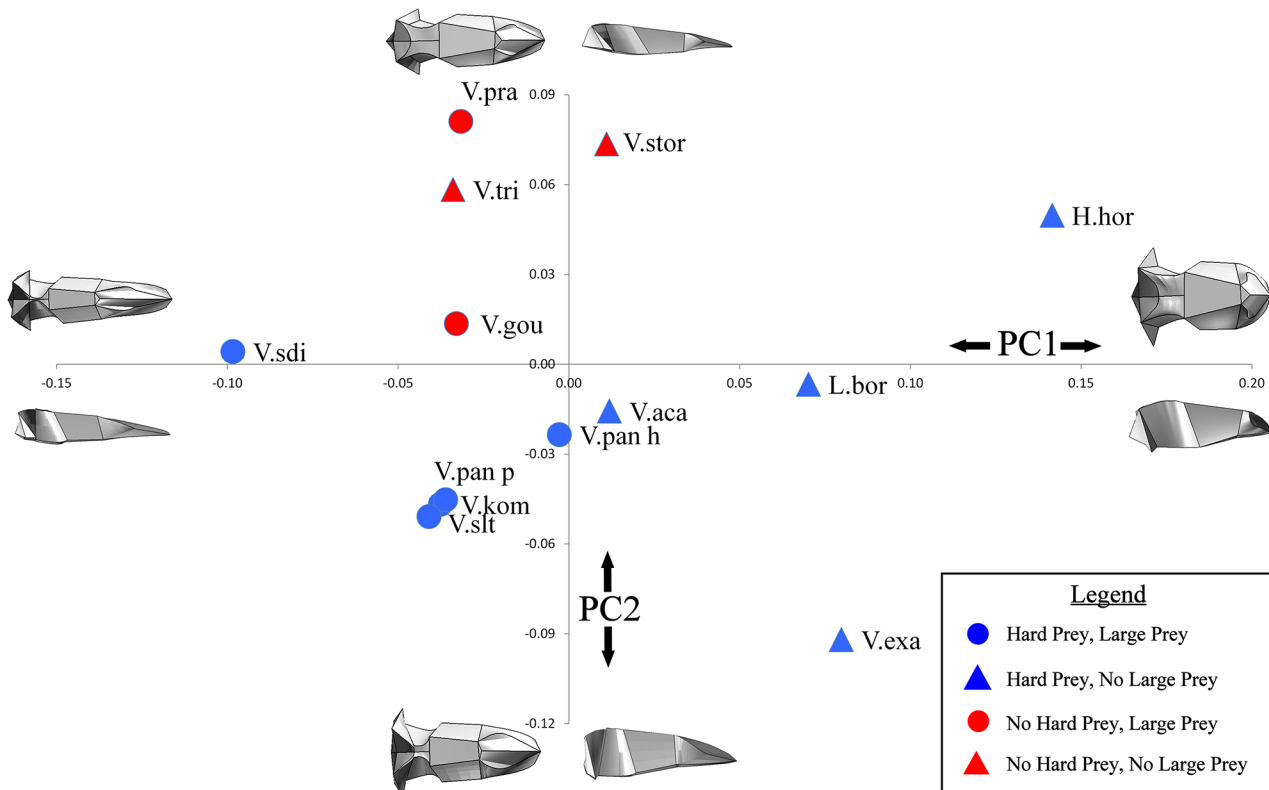
Fig 6. Cranial morphospace. Principal component plot of cranial morphospace. The diagrams at the end of each axis represent the theoretical geometry of the cranium in dorsal and lateral view. Each marker depicts the location of that specimen in morphospace as well as whether the animal was classed as feeding on hard prey (blue = yes, red = no) and whether the animal was classed as feeding on comparatively large prey (circle = yes, triangle = no). Abbreviations: H.hor, *Heloderma horridum;* L.bor, *Lanthanotus borneensis;* V.aca, *Varanus acanthurus;* V.exa, *Varanus exanthematicus;* V.gou, *Varanus gouldii;* V.kom, *Varanus komodoensis;* V.pan h, *Varanus panoptes horni;* V.pan p, *Varanus panoptes panoptes;* V.pra, *Varanus prasinus;* V.sdi, *Varanus salvadorii;* V.slt, *Varanus salvator;* V.stor, *Varanus storri;* V.tri, *Varanus tristis.*

doi:10.1371/journal.pone.0130625.g006

([Fig 10](#)). Within intrinsic (bite) loading strain was higher in the mandible than the cranium. In contrast extrinsic (shake and pull) load cases resulted in higher levels of strain in the cranium than the mandible. Overall the results show that each species varies considerably in terms of its ability to resist applied load and that, in some instances, the various structures are carrying load in different parts of the skull.

The relationship between morphology and performance

Comparisons between linear measurements of shape and performance showed that, within the cranium, tooth row length (TRL) was the best predictive variable for strain during bite and shake loading whilst dorsal cranial length (DCL) was the best predictive variable for pull loading. Mandible length (ML) was found to be the best predictor for strain levels during bite, shake and pull loading in the mandible ([Table 6](#)). In all cases larger values corresponded with higher levels of strain.

Partial least squares regression identified that the cranial shape was closely related to the response of models to bite and shake loading ([Table 7](#)). The relationships were however less strong in the mandible (Percentage variation explained for cumulative Y = 40.58 and 26.22 for the cranium and mandible respectively). In both the cranium and the mandible shake loading had a stronger relationship to shape than biting, and both of these were stronger than pulling
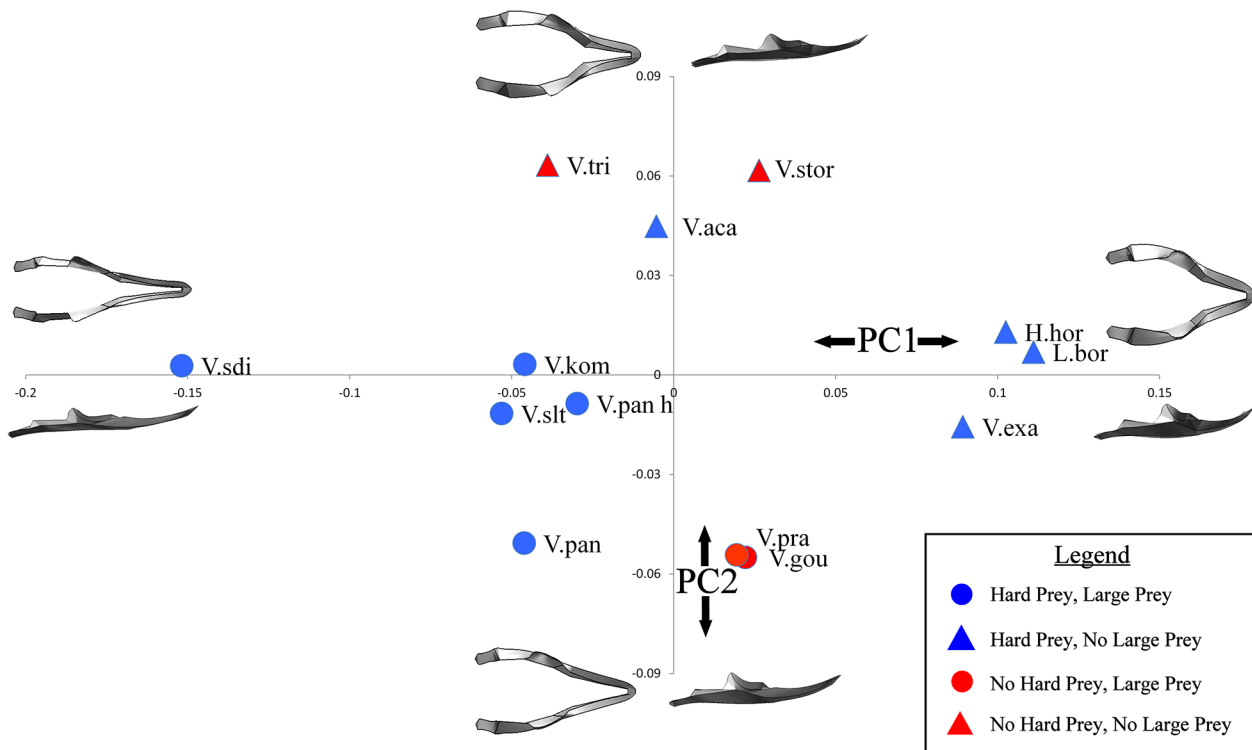
Fig 7. Mandibular morphospace. Principal component plot of mandibular morphospace. The diagrams at the end of each axis represent the theoretical geometry of the mandible in dorsal and lateral view. Each marker depicts the location of that specimen in morphospace as well as whether the animal was classed as feeding on hard prey (blue = yes, red = no) and whether the animal was classed as feeding on comparatively large prey (circle = yes, triangle = no). Abbreviations: H.hor, *Heloderma horridum;* L.bor, *Lanthanotus borneensis;* V.aca, *Varanus acanthurus;* V.exa, *Varanus exanthematicus;* V. gou, *Varanus gouldii;* V.kom, *Varanus komodoensis;* V.pan h, *Varanus panoptes horni;* V.pan p, *Varanus panoptes panoptes;* V.pra, *Varanus prasinus;* V.sdi, *Varanus salvadorii;* V.slt, *Varanus salvator;* V.stor, *Varanus storri;* V.tri, *Varanus tristis*.

doi:10.1371/journal.pone.0130625.g007

(Table 7). Variable Importance Values of 1.4130 and 1.4142 for the PC1 in the cranium and mandible respectively, and 0.0582 and 0.0068 for PC2 in the cranium and mandible respectively indicate that PC1 values were far more important in these relationships.

The relationship between performance and ecology

No relationships were observed between the presence of large prey in the diet of species and the structural performance of either the cranium or the mandible in any type of loading (Table 8). Relationships were observed between the presence of hard prey items within the diet of the species and the structural performance of cranial and mandible models; species that fed on hard prey items performed with less strain in bite loading than other species.

Discussion

We aimed to investigate the relationships between the cranial morphology, biomechanical performance (VM strain under biting, pulling and shaking loads) and feeding ecology of varanoid lizards. There were strong relationships between shape and performance; crania and mandibles with larger widths and heights (high PC1 values) performed better at biting and shaking. Further, there was some evidence for relationships between performance and diet; species that performed well in bite loading were also found to have hard prey within their diet. However, the relationships between morphology and performance were not as evident as that reported in
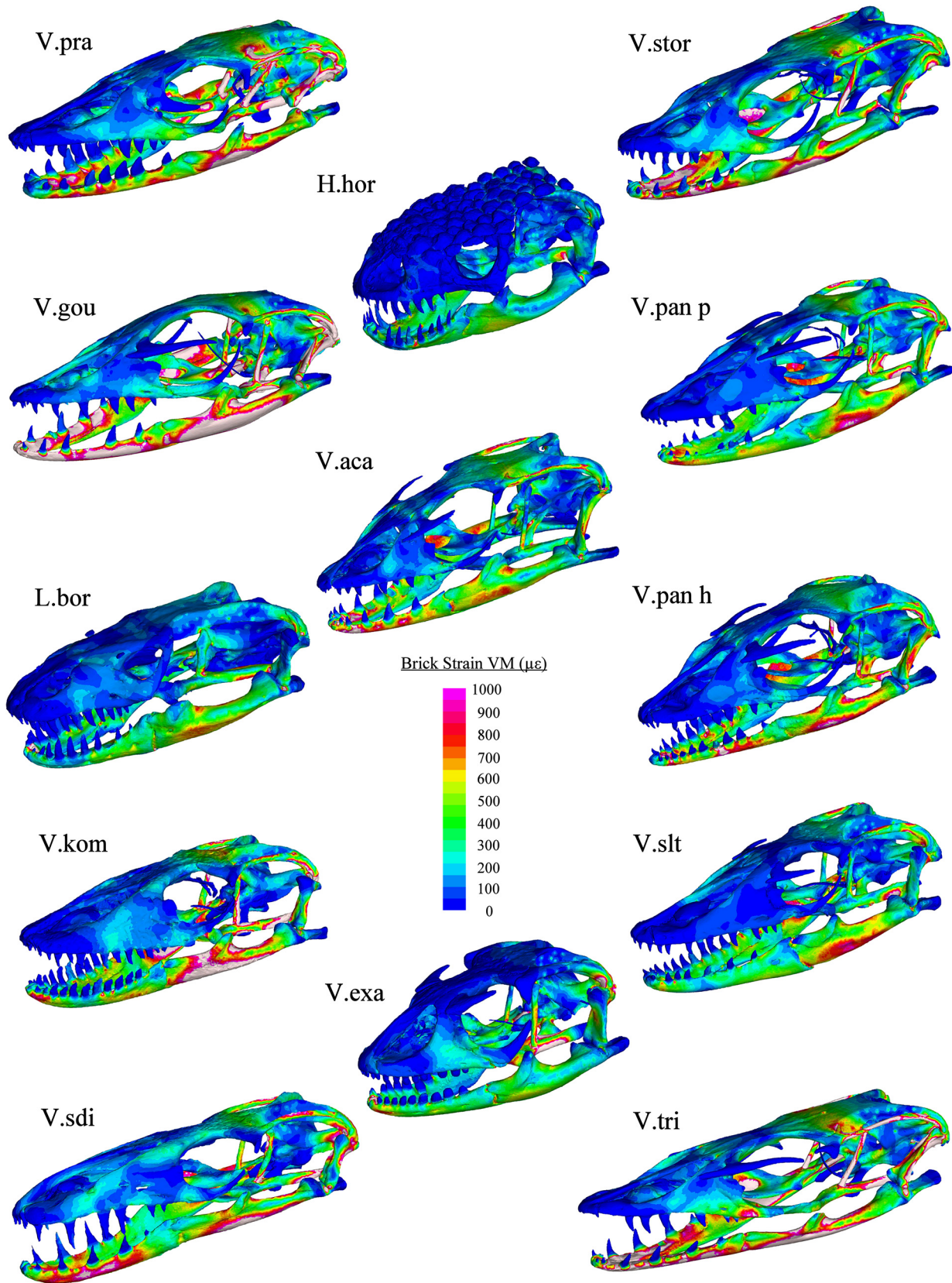
Brick Strain VM (με)

Fig 8. VM Strain plots: Bite loading. Cool colours (blues) represent areas of low stain, hot colours (reds) represent areas of high strain and white areas represent areas where the upper strain threshold (1000 με) was exceeded. Load was applied through muscle beams at a magnitude that standardised bite force at the teeth to 47.8 N (see S1 Table for muscle forces used for each model). Abbreviations: H.hor, *Heloderma horridum;* L.bor, *Lanthanotus borneensis;* V.aca, *Varanus acanthurus;* V.exa, *Varanus exanthematicus;* V.gou, *Varanus gouldii;* V.kom, *Varanus komodoensis;* V.pan h, *Varanus panoptes horni;* V.pan p, *Varanus panoptes panoptes;* V.pra, *Varanus prasinus;* V.sdi, *Varanus salvadorii;* V.slt, *Varanus salvator;* V.stor, *Varanus storri;* V.tri, *Varanus tristis.*

doi:10.1371/journal.pone.0130625.g008

previous studies [21,75], and did not match predictions from mechanical first principles, or those identified by FEA in other taxa [21].

Ecomorphology

Species that feed on large prey clustered together in the bottom right of both the cranial and mandible morphospace (gracile with long rostrum). Species that do not feed on hard prey items clustered in the centre top of cranial morphospace exhibiting low cranial height. There was a clear relationship between prey size and mandible shape, with macrophagous species having lower mandible PC1 and PC2 values. Phylogenetic patterns were also present, for example dwarf monitor (subgenus *Odatria*) mandibles clustered together in the morphospace.

The most extreme form of feeding upon hard prey is durophagy, *Varanus exanthematicus* and *L. borneensis* are both durophagous, feeding on hard prey items (molluscs and crabs respectively) [59,76]. *Heloderma horridum*, although not distinctively durophagous, does also feed on harder prey items such as eggs. These three species have the highest PC1 scores for both crania and mandibles (Figs 6 & 7), indicating that, as expected, the shortest and most robust skulls are those suited for durophagy. Note, however, that phylogeny is also important here; durophagy may be a plesiomorphic trait of the varanoid lizards as *Varanus exanthematicus* and *L. borneensis* are basal species.

Loading type

In simulations of biting, the models consistently showed higher strain levels in the mandible than the cranium. Biomechanical performance during biting may thus be limited primarily by mandibular morphology, as has been suggested in previous analyses [77]. This may also be a result of differing evolutionary forces influencing the two structures; as the cranium houses the brain and capsules, its morphology is a result of multivariate selection, whereas the mandible is principally involved in feeding [78]. The high strain levels observed in the brain case and in between the orbits during shake loading indicate that these areas may be important in this behaviour (Fig 9). This raises the possibility of a trade-off between eye size (sensory function) and strength during shaking (structural function), consistent with a previous study on theropod dinosaurs [79]. The two sub-adult specimens included within the analysis (*V. komodoensis* and *V. gouldii)* exhibited higher magnitudes of strain than most other specimens. Eyes are proportionately larger in juveniles, leaving less space for bone in the interorbital region, and that region exhibits high level of strain during biting and shaking. Thus fine scale structural characteristics such as allometric differences between juveniles and adults may be of particular importance to trade-offs in cranial structural performance and neurocranial anatomy.

We examined correlations between morphology and performance using two measures of morphology: linear (euclidean distances), and multivariate (geometric morphometrics).

Linear morphometrics vs performance

Walmsley et al. (2013) found that relationships between linear morphometrics and performance match well with predictions from mechanical first principles in a comparative analysis of crocodile mandibles. However, relationships between linear measures of shape and
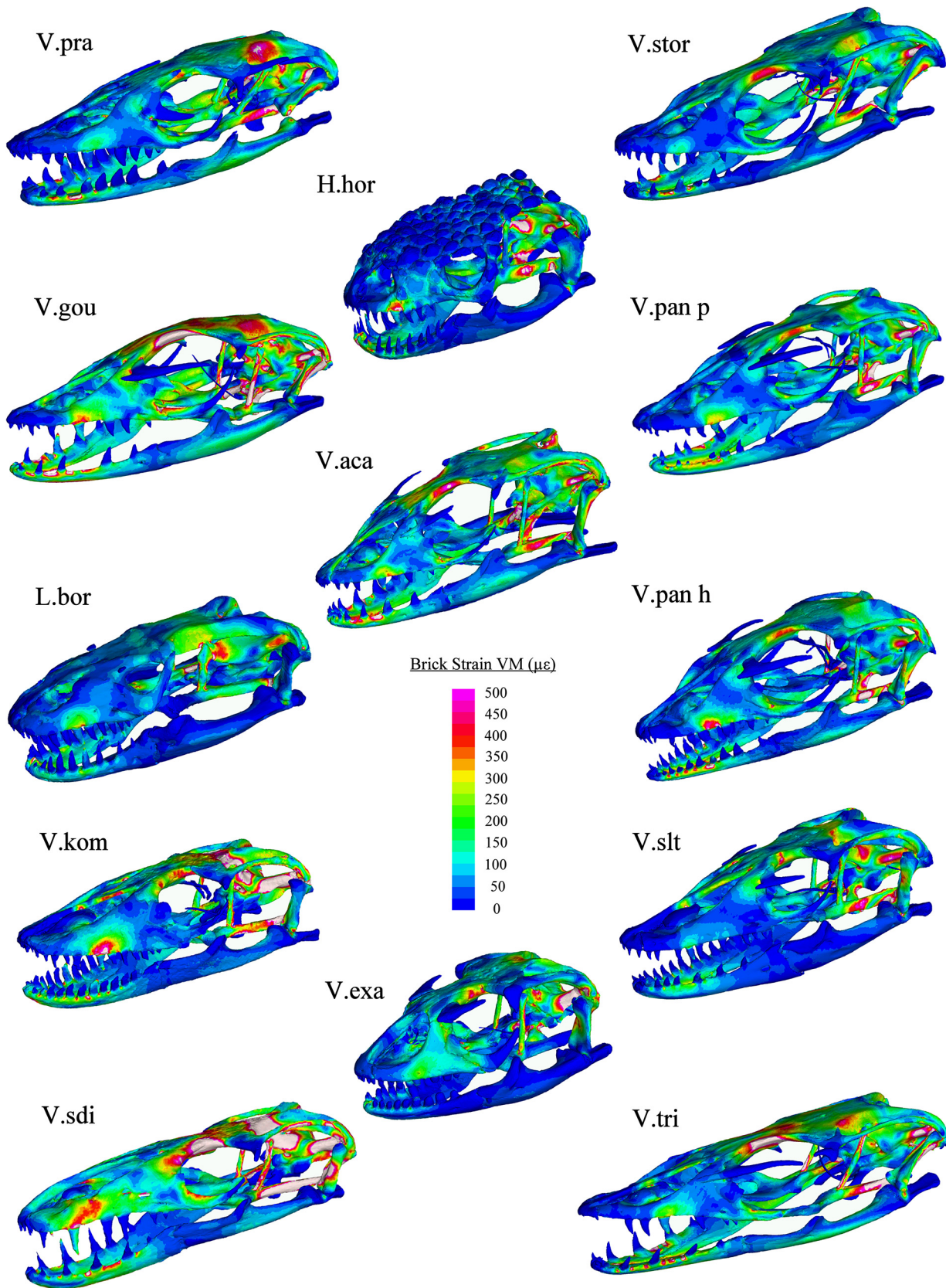
Brick Strain VM (με)

500
450
400
350
300
250
200
150
100
50
0

Fig 9. VM Strain plots: Shake loading. Cool colours (blues) represent areas of low stain, hot colours (reds) represent areas of high strain and white areas represent areas where the upper strain threshold (500 με) was exceeded. An arbitrary load of 20N was applied laterally through H beams connecting the four middle teeth. Abbreviations: H.hor, *Heloderma horridum;* L.bor, *Lanthanotus borneensis;* V.aca, *Varanus acanthurus;* V.exa, *Varanus exanthematicus;* V.gou, *Varanus gouldii;* V.kom, *Varanus komodoensis;* V.pan h, *Varanus panoptes horni;* V.pan p, *Varanus panoptes panoptes;* V.pra, *Varanus prasinus;* V.sdi, *Varanus salvadorii;* V.slt, *Varanus salvator;* V.stor, *Varanus storri;* V.tri, *Varanus tristis.*

performance results from FEA in our study were inconsistent with our predictions: the length of the tooth row and mandible correlated better with skull strength (Table 6) than the measures we hypothesised a priori (i.e. rostral/mandibular height for biting, rostral/mandibular width for shaking, and the combination of cranial/mandibular height and width for pull back loads).

Multivariate morphometrics and performance

In the principle components analysis of skull shape, PC1 values correlated negatively with skull length and positively with skull width, so that species with high PC1 values had shorter, wider skulls with taller snouts (Figs 3 and 4). *A priori*, these would be expected to be stronger under biting and especially shaking loads, and the results agree; two blocked partial least squares regression showed that crania and mandibles with high PC1 values performed better than others, particularly in bite and shake loading (Table 7). Species with lower PC2 values have taller skulls post-orbitally, which is also expected to increase skull strength, but this had a smaller influence on strain levels as indicated by comparable lower variable importance values in the 2-block partial least squares analysis. The fact that there were higher explanation values for biting and shaking load cases may mean that performance in these behaviours is more important than performance in pulling behaviours in driving patterns of morphological variation in the varanoid skull.

Overall

The apparent mismatch between the linear measurements that were predicted to influence skull performance, and those that actually do, may relate to the space frame structure of the varanoid lizard cranial system [36]. Compared with the shell constructions, it seems that the performance of varanoid skulls is difficult to predict from simple measurements chosen with reference to basic beam theory. However, more complex multivariate measures of skull shape do show correlations with performance that make sense in terms of fundamental mechanical principles. If this is the case, then the landmarks used in the multivariate measures must somewhere incorporate aspects of shape that do influence performance. The higher correlation between morphology and performance in the cranium than in the mandible may indicate that the cranium is under a higher selective pressure for strength; intuitively this is difficult to understand as cranial morphology is expected to represent compromise between various functional demands (feeding, protecting the brain, olfaction etc.) whilst the mandible primarily functions in feeding [78].

V. komodoensis exhibited high levels of strain to bite, shake and pull loading. This result is may be a consequence of our model being constructed from a sub-adult specimen (a size that cannot exploit large prey) that has no ecological need for a robust skull. Alternatively it is also possible that the use of toxic effects (whether produced by bacteria or venom glands) to incapacitate prey may free the Komodo dragon from the need to have a highly robust skull [45,80,81]. Clearly further research that measures cranial performance across ontogeny may detail allometric changes in performance consistent with dietary transitions from small prey in hatchlings to large ungulates (e.g. water buffalo) in adults [82].
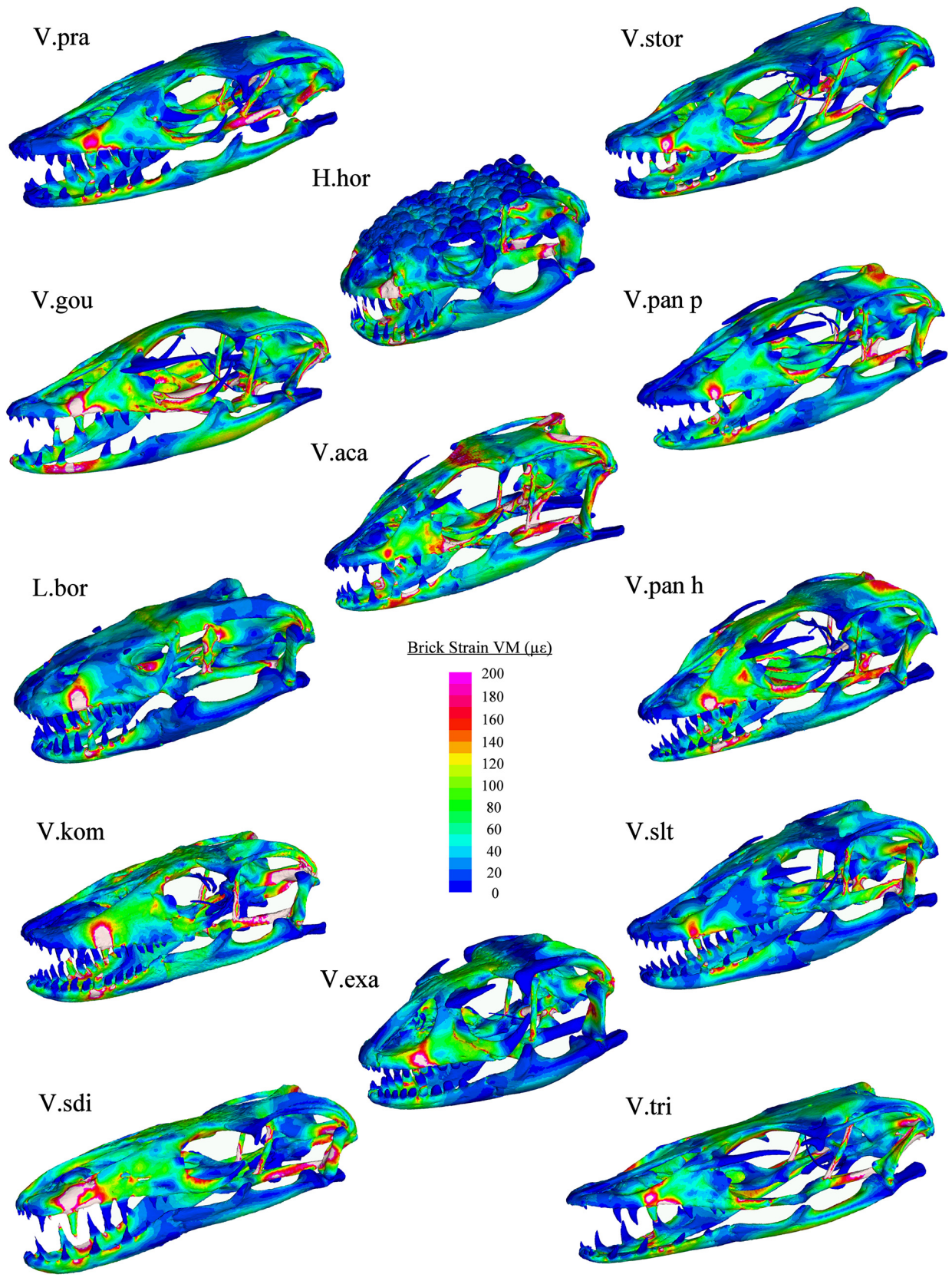
Brick Strain VM (με)

Fig 10. VM Strain plots: Pull loading. Cool colours (blues) represent areas of low stain, hot colours (reds) represent areas of high strain and white areas represent areas where the upper strain threshold (200 με) was exceeded. An arbitrary load of 30N was applied anteriorly through H beams connecting the four middle teeth. Abbreviations: H.hor, *Heloderma horridum;* L.bor, *Lanthanotus borneensis;* V.aca, *Varanus acanthurus;* V.exa, *Varanus exanthematicus;* V. gou, *Varanus gouldii;* V.kom, *Varanus komodoensis;* V.pan h, *Varanus panoptes horni;* V.pan p, *Varanus panoptes panoptes;* V.pra, *Varanus prasinus;* V.sdi, *Varanus salvadorii;* V.slt, *Varanus salvator;* V.stor, *Varanus storri;* V.tri, *Varanus tristis.*

doi:10.1371/journal.pone.0130625.g010

Do macropredaceous varanoids have longer, weaker skulls?

Species that fed on large prey items compared to their size possess unique morphological characteristics such as elongate crania and mandibles. Predatory mammals and crocodiles that feed on large prey exhibit the opposite trend with shorter, more robust cranial structures [24,75]. This may be due to the influence of other performance considerations such as the need for a long mandible to better tear flesh during pull back prey processing. At least some of the varanid species that feed on large prey use pull back behaviours to process their food. In *V. komodoensis* the tooth row acts as a saw blade which cuts food as the teeth are drawn back [15]. Logically, an elongate mandible can carry more teeth and thus increases the efficiency of prey processing. Many of these species also feed on carrion which may mean that the skull does not need to handle the same level of extrinsic forces that can occur in high levels during prey capture [59]. Alternatively the elongate skulls could prove useful in allowing the predator to better access hard to reach parts of the carcass.

Methodological limitations and agenda for future research

The complexity of varanoid morphology, behaviour and ecology represented a significant challenge for this study. The relationships identified between morphology and performance were not as strong as those identified in other taxonomic groups [21,24,75]. Either there is only a weak link between morphology, performance and ecology within the group (with behaviour acting as a wild card), or there are limitations on the approach that we used here.

Sample size. Many previous FEA studies have characterised the biomechanics of a single specimen or qualitatively compared between a small number of species [25,26,27,37,45,48]. The complex morphological differences that exist between the varanoid specimens mean that a higher number of individuals are more suitable to tease apart the relationship between form and function. Additionally, a limited sample size prevents us from characterising the effects of intraspecific variation such as allometry or sexual dimorphism. Ontogenetic changes in skull shape have been shown to be large within some varanid species [83]. Sample size thus represents a substantial hurdle for the area of ecological biomechanics given that finite element models take considerable time to produce.

Structural complexity. The space-frame nature of the varanoid cranial system represented another significant challenge for this study. The strength of a structure is dependent on many characteristics of the shape such as the thickness of bones or their orientation. Gross morphology was found to have a large influence (PC 1 correlated with some measures of performance). However, subtler morphological characteristics, such as thicknesses of particular struts, that were not measured, are likely to also be important in dictating strength. It is logical that finer morphological characteristics also play a larger role in dictating strength in space frame structures compared to shell structures. This is because space-frame structures rely on fine scale and localised morphological features more than shell structures that distribute load across a wide surface. Sutures were not included in the analysis; these features have been found to have considerable influence on FEA results in previous studies [40,49,84,85,86,87]. Due to a lack of information on the nature and extent of cranial kinesis (movement between the bones of the cranium) in varanoids it was excluded in FEA models and it is likely that this has also
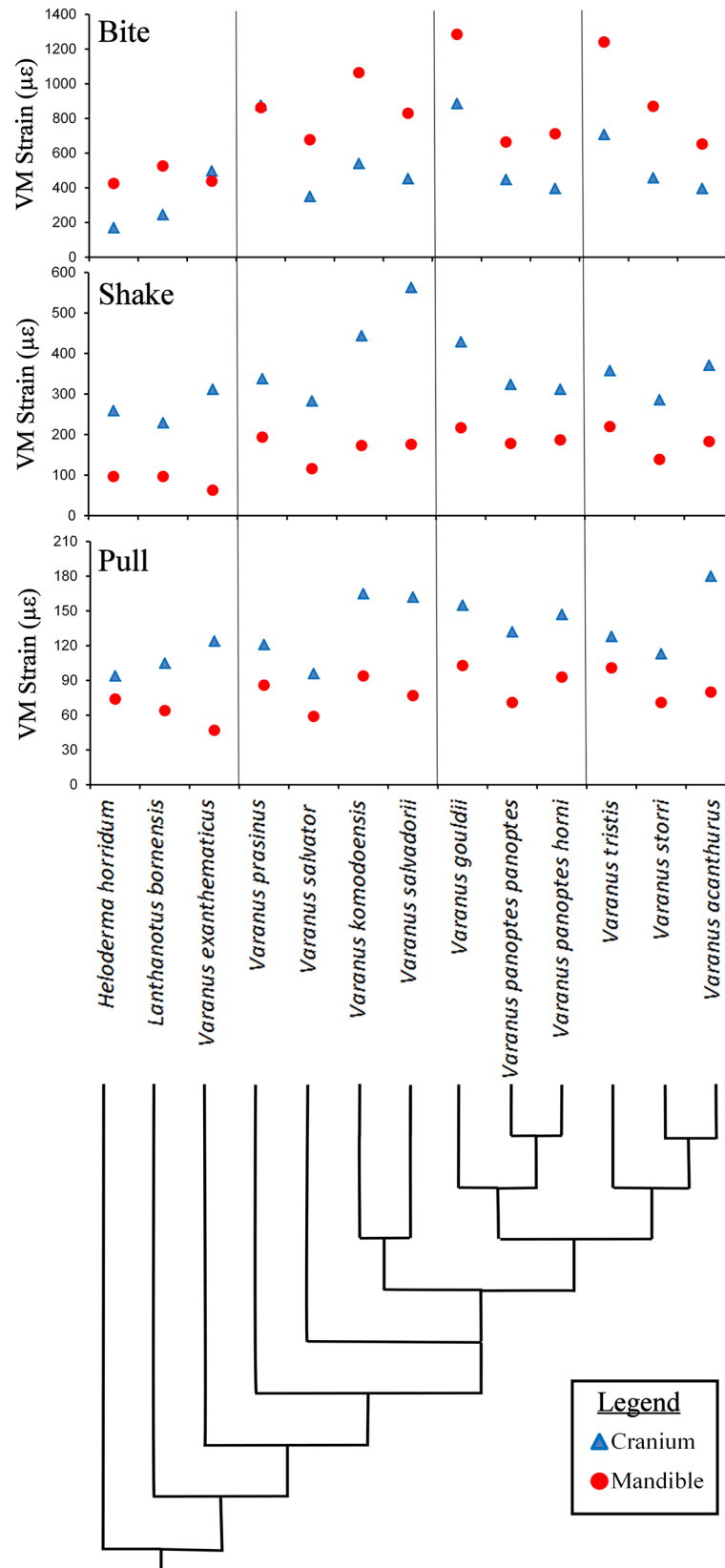
Fig 11. Magnitudes of strain. Comparative performance (95% von Mises strain levels) of the cranium (blue) and mandible (red) models in bite, shake and pull loading. The species are in phylogenetic order with a simplified phylogenetic tree based on Vidal [11] showing the relative position of each species.

doi:10.1371/journal.pone.0130625.g011

Table 6. Best linear morphometric predictor variables for each load case.

Cranium				Mandible			
Load Case	Best Predictor	n.o of factors	% explained	Load Case	Best Predictor	n.o of factors	% explained
Bite	TRL	1	90.24	Bite	ML	1	69.96
Shake	TRL	1	92.11	Shake	ML	1	81.99
Pull	DCL	1	83.28	Pull	ML	1	65.68

doi:10.1371/journal.pone.0130625.t006

Table 7. Statistical comparison (PLS) between morphology (PC1 and PC2) and Performance (Bite, Shake and Pull load cases).

Cranium	n.o of factors	% explained	Mandible	n.o of factors	% explained
Bite	1	41.02	Bite	1	27.87
Shake	1	52.19	Shake	1	38.46
Pull	1	28.53	Pull	1	12.34

doi:10.1371/journal.pone.0130625.t007

Table 8. Univariate Statistical comparison (ANOVA) between ecological class and performance in each load case.

Cranium			Mandible		
Hard		Prob>F	Hard		Prob>F
	Bite	**0.0106**		Bite	**0.0064**
	Shake	0.7469		Shake	0.1207
	Pull	0.9016		Pull	0.1083
Large		Prob>F	Large		Prob>F
	Bite	0.1788		Bite	0.1636
	Shake	0.0887		Shake	0.0886
	Pull	0.2995		Pull	0.2660

doi:10.1371/journal.pone.0130625.t008

influenced the results to some degree. The low percentage of total variance explained by the PC analyses could also be due to the occurrence of cranial kinesis which would alter the relative position of landmarks between specimens.

Muscle anatomy. Because detailed data on muscle activation and anatomy was not available for the majority of these species we were forced to assume that all species possess identical muscle attachment sites and that each muscle is used at the same time in biting. This may not be a realistic assumption; it would be useful for future studies to address the function of specific muscles and the role of muscle activation patterns.

Loading conditions. Recent sensitivity studies have identified that biological assumptions may have more influence on FEA results then those about material properties or scaling [57]. As no kinematic data was collected for this study it is possible that the forces applied were not exactly biologically equivalent. Future studies should aim to collect data on the exact loading conditions encountered in each species through observation of either wild or captive animals.

Ecological data. The performance and shape data used in this study are fine grained whereas the ecological data are quite course, with only qualitative categories being drawn. It is possible (even likely) that clear relationships between skull shape, biomechanics and ecology do exists but that fine scale ecological data are required to demonstrate them statistically. However this hypothesis cannot be tested without improving the available ecological data, and so quantitative studies of varanid ecology are a priority for investigating form-function relationships in this taxon.

Performance metrics. Within this study we have only examined strength (limited to three load cases) as a performance measure. As a complex integrated system other factors such as the ability of the skull to protect vital organs, the ability of the cranial system to produce bite forces and for certain sensory organs to function, are likely to also influence the shape of the skull [88].

Conclusions

This study identifies that varanoid lizards do exhibit considerable variation in cranial and mandibular morphology that has specific influences on structural performance during biologically relevant loading. This could be an important characteristic that allows for these closely related taxa to exploit diverse ecological habits. The relationships between the morphology of varanoid lizard skulls, their structural performance and their ecology are not as would be predicted from our previous knowledge of cranial form and function. The space frame structure of the varanoid lizard skull as well as the unique behaviours that are used by these species to capture and process prey items may be the cause of this discrepancy. It is hoped that the insights gained from this study will help to guide future research on space-frame skull structures and more broadly in the area of ecological biomechanics. The results may also provide useful context for future paleobiological studies on taxa such as theropod dinosaurs that may use varanoids as extant morphological analogues.

Supporting Information

S1 File. Measurement definitions and Landmark locations.
(DOCX)

S2 File. Supplementary section containing R code for statistical analysis.
(TXT)

S3 File. Instructions on the use of the R code used to generate statistical summaries.
(RTF)

S1 Table. Supplementary data on muscle forces applied to models. Natural forces represent the force per truss element predicted for each of the muscle beams based on muscle cross sectional area at natural size. Adjusted forces represent the force per truss element adjusted so that the models produced the same node reaction force at the bite location in volume scaled models. Total muscle forces represent the total force applied to each model to generate the same node reaction forces at bite location.
(XLSX)

Acknowledgments

Author Contributions

Conceived and designed the experiments: MRM MM PDC SW CRM. Performed the experiments: MRM. Analyzed the data: MRM MRQ CWW MM TSJ CRM. Contributed reagents/materials/analysis tools: CRM PDC SW HR. Wrote the paper: MRM MM PDC MRQ CWW TSJ SW CRM HR.

References

1. Fitch AJ, Goodman AE, Donnellan SC. A molecular phylogeny of the Australian monitor lizards (Squamata: Varanidae) infered from mitochondrial DNA sequences. Australian Journal of Zoology. 2006; 54:253–69.

2. Pianka ER, King DR, King RA. Varanoid lizards of the world: Indiana University Press; 2004.

3. Pianka ER. Comparative ecology of *Varanus* in the Great Victoria Desert. Australian Journal of Ecology. 1994; 19:395–408.

4. Pianka ER. Evolution of body size: varanid lizards as a model system. American Naturalist. 1995:398–414.

5. Clemente CJ, Withers PC, Thompson G, Lloyd D. Evolution of limb bone loading and body size in varanid lizards. The Journal of Experimental Biology. 2011; 214(18):3013–20. doi: 10.1242/jeb.059345

6. Thompson GG, Withers PC. Comparative Morphology of Western Australian Varanid Lizards (Squamata: Varanidae). Journal of Morphology. 1997; 233:127–52.

7. Stayton TS. Morphological evolution of the lizard skull: A geometric morphometrics survey. Journal of Morphology. 2005; 263:47–59. PMID: 15536647

8. Clemente CJ, Thompson GG, Withers PC. Evolutionary relationships of sprint speed in Australian varanid lizards. Journal of Zoology. 2009; 278(4):270–80. doi: 10.1111/j.1469-7998.2009.00559.x

9. Openshaw G, Keogh J. Head shape evolution in monitor lizards (Varanus): interactions between extreme size disparity, phylogeny and ecology. Journal of Evolutionary Biology. 2014; 27(2):363–73. doi: 10.1111/jeb.12299 PMID: 24386920

10. Ast JC. Mitochondrial DNA evidence and evolution in Varanoidea (Squamata). Cladistics. 2001; 17(3):211–26.

11. Vidal N, Marin J, Sassi J, Battistuzzi FU, Donnellan S, Fitch AJ, et al. Molecular evidence for an Asian origin of monitor lizards followed by Tertiary dispersals to Africa and Australasia. Biology Letters. 2012; 8(5):853–5. doi: 10.1098/rsbl.2012.0460 PMID: 22809723

12. Jones ME, Anderson CL, Hipsley CA, Müller J, Evans SE, Schoch RR. Integration of molecules and new fossils supports a Triassic origin for Lepidosauria (lizards, snakes, and tuatara). BMC evolutionary biology. 2013; 13(1):208.

13. Reeder TW, Townsend TM, Mulcahy DG, Noonan BP, Wood PL Jr., Sites JW Jr., et al. Integrated Analyses Resolve Conflicts over Squamate Reptile Phylogeny and Reveal Unexpected Placements for Fossil Taxa. PLOS one. 2015; 10(3):e0118199. doi: 10.1371/journal.pone.0118199 PMID: 25803280

14. Loop MS. The Effect of Relative Prey Size on the Ingestion Behavior of the Bengal Monitor, *Varanus bengalensis* (Sauria: Varanidae). Herpetologica. 1974; 30(2):123–7. doi: 10.2307/3892027

15. D'Amore DC, Blumenschine RJ. Komodo monitor (*Varanus komodoensis*) feeding behavior and dental function reflected through tooth marks on bone surfaces, and the application to ziphodont paleobiology. Paleobiology. 2009; 35(4):525–52.

16. D'Amore DC, Moreno K, McHenry CR, Wroe S. The effects of biting and pulling on the forces generated during feeding in the Komodo Dragon (*Varanus komodoensis*). PLOS one. 2011; 6(10):e26226. doi: 10.1371/journal.pone.0026226 PMID: 22028837

17. Wainwright PC. Functional morphology as a tool in ecological research. Ecological morphology. 1994:42–59.

18. Rayfield EJ. Finite element analysis and understanding the biomechanics and evolution of living and fossil organisms. Annual Review of Earth and Planetary Sciences. 2007; 35:541–76.

19. Parr W, Wroe S, Chamoli U, Richards H, McCurry M, Clausen P, et al. Toward integration of geometric morphometrics and computational biomechanics: New methods for 3D virtual reconstruction and quantitative analysis of Finite Element Models. Journal of Theoretical Biology. 2012; 301:1–14. doi: 10.1016/j.jtbi.2012.01.030 PMID: 22342680

20. O'Higgins P, Cobb SN, Fitton LC, Gröning F, Phillips R, Liu J, et al. Combining geometric morphometrics and functional simulation: an emerging toolkit for virtual functional analyses. Journal of Anatomy. 2011; 218(1):3–15. doi: 10.1111/j.1469-7580.2010.01301.x PMID: 20880075

21. Walmsley CW, Smits PD, Quayle MR, McCurry MR, Richards HS, Oldfield CC, et al. Why the Long Face? The Mechanics of Mandibular Symphysis Proportions in Crocodiles. PLOS ONE. 2013; 8(1): e53873. doi: 10.1371/journal.pone.0053873 PMID: 23342027

22. Pierce SE, Angielczyk KD, Rayfield EJ. Patterns of morphospace occupation and mechanical performance in extant crocodilian skulls: a combined geometric morphometric and finite element modeling approach. Journal of morphology. 2008; 269(7):840–64. doi: 10.1002/jmor.10627 PMID: 18496856

23. Piras P, Maiorino L, Teresi L, Meloro C, Lucci F, Kotsakis T, et al. Bite of the Cats: Relationships between Functional Integration and Mechanical Performance as Revealed by Mandible Geometry. Systematic biology. 2013; 62(6):878–900. doi: 10.1093/sysbio/syt053 PMID: 23925509

24. McHenry CR, Clausen PD, Daniel WJ, Meers MB, Pendharkar A. Biomechanics of the rostrum in crocodilians: A comparative analysis using finite-element modeling. The Anatomical Record Part A. 2006; 288:827–49.

25. Wroe S, Clausen P, McHenry C, Moreno K, Cunningham E. Computer simulation of feeding behaviour in the thylacine and dingo: a novel test for convergence and niche overlap. Proceedings of the Royal Society Series B. 2007; 274:2819–28. doi: 10.1098/rspb.2007.0906

26. Wroe S, Ferrara TL, McHenry C, Curnoe D, Chamoli U. The craniomandibular mechanics of being human. Proceedings of the Royal Society of London B. 2010; 277:3579–86.

27. McHenry CR, Wroe S, Clausen PD, Moreno K, Cunningham E. Supermodeled sabercat, predatory behavior in *Smilodon fatalis* revealed by high-resolution 3D computer simulation. Proceedings of the National Academy of Sciences. 2007; 104(41):16010–5.

28. Tseng ZJ, Stynder D. Mosaic functionality in a transitional ecomorphology: skull biomechanics in stem Hyaeninae compared to modern South African carnivorans. Biological Journal of the Linnean Society. 2011; 102(3):540–59.

29. Tseng ZJ. Testing Adaptive Hypotheses of Convergence with Functional Landscapes: A Case Study of Bone-Cracking Hypercarnivores. PLOS one. 2013; 8(5):e65305. doi: 10.1371/journal.pone.0065305 PMID: 23734244

30. Lautenschlager S, Witmer LM, Altangerel P, Rayfield EJ. Edentulism, beaks, and biomechanical innovations in the evolution of theropod dinosaurs. Proceedings of the National Academy of Sciences. 2013. 110; 51: 20657–20662. doi: 10.1073/pnas.1310711110

31. Soons J, Herrel A, Genbrugge A, Aerts P, Podos J, Adriaens D, et al. Mechanical stress, fracture risk and beak evolution in Darwin's ground finches (Geospiza). Philosophical Transactions of the Royal Society B: Biological Sciences. 2010; 365(1543):1093–8. doi: 10.1098/rstb.2009.0280 PMID: PMC2830229.

32. Ross CF, Berthaume MA, Dechow PC, Iriarte-Diaz J, Porro LB, Richmond BG, et al. In vivo bone strain and finite-element modeling of the craniofacial haft in catarrhine primates. Journal of Anatomy. 2011; 218(1):112–41. doi: 10.1111/j.1469-7580.2010.01322.x PMID: 21105871

33. Slater GJ, Van Valkenburgh B. Allometry and performance: the evolution of skull form and function in felids. Journal of Evolutionary Biology. 2009; 22(11):2278–87. doi: 10.1111/j.1420-9101.2009.01845.x PMID: 19796083

34. Dumont ER, Piccirillo J, Grosse IR. Finite-element analysis of biting behavior and bone stress in the facial skeletons of bats. The Anatomical Record Part A. 2005; 283A:319–30.

35. Snively E, Cox A. Structural mechanics of pachycephalosaur crania permitted head-butting behavior. Palaeontologia Electronica. 2008; 11(1):3A.

36. Moreno K, Wroe S, Clausen P, McHenry C, D'Amore DC, Rayfield EJ, et al. Cranial performance in the Komodo dragon (*Varanus komodoensis*) as revealed by high-resolution 3-D finite element analysis. Journal of Anatomy. 2008; 212(6):736–46. doi: 10.1111/j.1469-7580.2008.00899.x PMID: 18510503

37. Wroe S. Cranial mechanics compared in extinct marsupial and extant african lions using a finite-element approach. Journal of Zoology. 2008; 274:332–9.

38. Bourke J, Wroe S, Moreno K, McHenry C, Clausen P. Effects of gape and tooth position on bite force and skull stress in the dingo (Canis lupus dingo) using a 3-dimensional finite element approach. PLOS One. 2008; 3(5):e2200. doi: 10.1371/journal.pone.0002200 PMID: 18493603

39. Oldfield CC, McHenry CR, Clausen PD, Chamoli U, Parr WCH, Stynder DD, et al. Finite element analysis of ursid cranial mechanics and the prediction of feeding behaviour in the extinct giant *Agriotherium africanum*. Journal of Zoology. 2012; 286(2):163–170. doi: 10.1111/j.1469-7998.2011.00862.x

40. Bright JA. The Importance of Craniofacial Sutures in Biomechanical Finite Element Models of the Domestic Pig. PLOS one. 2012; 7(2):e31769. doi: 10.1371/journal.pone.0031769 PMID: 22363727

41. Chalk J, Richmond BG, Ross CF, Strait DS, Wright BW, Spencer MA, et al. A finite element analysis of masticatory stress hypotheses. American Journal of Physical Anthropology. 2011; 145(1):1–10. doi: 10.1002/ajpa.21416 PMID: 21484756

42. Wang Q, Wright BW, Smith A, Chalk J, Byron CD. Mechanical Impact of Incisor Loading on the Primate Midfacial Skeleton and its Relevance to Human Evolution. The Anatomical Record: Advances in Integrative Anatomy and Evolutionary Biology. 2010; 293(4):607–17. doi: 10.1002/ar.21123

43. Curtis N, Witzel U, Fitton L, O'Higgins P, Fagan M. The Mechanical Significance of the Temporal Fasciae in Macaca fascicularis: An Investigation Using Finite Element Analysis. The Anatomical Record: Advances in Integrative Anatomy and Evolutionary Biology. 2011; 294(7):1178–90. doi: 10.1002/ar.21415

44. Dumont ER, Davis JL, Grosse IR, Burrows AM. Finite element analysis of performance in the skulls of marmosets and tamarins. Journal of Anatomy. 2011; 218(1):151–62. doi: 10.1111/j.1469-7580.2010.01247.x PMID: 20572898

45. Moreno K, Wroe S, Clausen P, McHenry C, D'Amore DC, Rayfield E, et al. Cranial performance in the Komodo dragon (*Varanus komodoensis*) as revealed by high-resolution 3-D finite element analysis. Journal of Anatomy. 2008; 212(6):736–46. doi: 10.1111/j.1469-7580.2008.00899.x PMID: 18510503

46. Curtis N, Jones MEH, Shi J, O'Higgins P, Evans SE, Fagan MJ. Functional Relationship between Skull Form and Feeding Mechanics in *Sphenodon*, and Implications for Diapsid Skull Development. PLOS one. 2011; 6(12):e29804. doi: 10.1371/journal.pone.0029804 PMID: 22216358

47. Rayfield EJ, Norman DB, Horner CC, Horner JR, Smith PM, Thomason JJ, et al. Cranial design and function in a large theropod dinosaur. Nature. 2001; 409:1033–7. PMID: 11234010

48. Rayfield E. Cranial mechanics and feeding in *Tyrannosaurus rex*. Proceedings of the Royal Society of London B. 2004; 271:1451–9.

49. Rayfield EJ. Using finite-element analysis to investigate suture morphology: A case study using large carnivorous dinosaurs. The Anatomical Record Part A. 2005; 283:349–65.

50. Richards R Jr. Principles of solid mechanics: CRC Press; 2010.

51. McNeel. Rhino3d.

52. Wiley D. Landmark Editor 3.0. Institute for Data Analysis and Visualization. Davis: University of California; 2006.

53. O'Higgins P, Jones N. Morphologika 2, v. 2.4. Hull York Medical School, York. 2006.

54. Erickson GM, Catanese J, Keaveny TM. Evolution of the biomechanical material properties of the femur. The Anatomical Record. 2002; 268(2):115–24. doi: 10.1002/ar.10145 PMID: 12221717

55. Holliday CM. New insights Into dinosaur jaw muscle anatomy. The Anatomical Record: Advances in Integrative Anatomy and Evolutionary Biology. 2009; 292(9):1246–65. doi: 10.1002/ar.20982

56. McHenry C. Devourer of Gods: the palaeology of the Cretaceous pliosaur Kronosaurus queenslandicus. Newcastle, NSW, Australia: University of Newcastle; 2009. http://hdl.handle.net/1959.13/935911

57. Walmsley CW, McCurry MR, Clausen PD, McHenry CR. Beware the black box: investigating the sensitivity of FEA simulations to modelling factors in comparative biomechanics. Peer J. 2013. doi: 10.7717/peerj.204

58. King D. The diet and foraging strategy of *Varanus acanthurus*. Biawak. 2008; 2(1):11–7.

59. Losos JB, Greene HW. Ecological and evolutionary implications of diet in monitor lizards. Biological Journal of the Linnean Society. 1988; 35:379–407.

60. Shine R. Food Habits, Habitats and Reproductive Biology of Four Sympatric Species of Varanid Lizards in Tropical Australia. Herpetologica. 1986; 42(3):346–60. doi: 10.2307/3892313

61. Beck D. Heloderma horridum. In: Pianka ER, King DR, King RA, editors. Varanoid lizards of the world. Bloomington: Indiana University Press; 2004. p. 521–7.

62. Dryden G. Varanus acanthurus. In: Pianka ER, King DR, King RA, editors. Varanoid lizards of the world. Bloomington: Indiana University Press; 2004. p. 298–307.

63. Thompson G. Varanus gouldii. In: Pianka ER, King DR, King RA, editors. Varanoid Lizards of the World. Bloomington Indiana University Press; 2004. p. 380–400.

64. Horn H-G. Varanus salvadorii. In: Pianka ER, King DR, King RA, editors. Varanoid lizards of the world. Bloomington Indiana University Press; 2004. p. 231–3.

65. Bennett D. Observations of Bosc's monitor lizard (*Varanus exanthematicus*) in the wild. Bull Chicago Herpetol Soc. 2002; 35:177–80.

66. Bennett D. Varanus exanthematicus. In: Pianka ER, King DR, King RA, editors. Varanoid lizards of the world. Bloomington Indiana University Press; 2004. p. 95–103.

67. Christian K. Varanus panoptes. In: Pianka ER, editor. Varanoid lizards of the world. Bloomington: Indiana University Press; 2004. p. 423–9.

68. Eidenmuller B. Varanus storri. In: Pianka ER, King DR, King RA, editors. Varanoid lizards of the world. Bloomington: Indiana University Press; 2004. p. 472–6.

69. Gaulke M, Horn H-G. Varanus salvator. In: Pianka ER, King DR, King RA, editors. Varanoid lizards of the world. Bloomington: Indiana University Press; 2004. p. 244–57.

70. Greene HW. Varanus prasinus. In: Pianka ER, King DR, King RA, editors. Varanoid lizards of the world. Bloomington: Indiana University Press; 2004. p. 225–39.

71. Shannon R, Mendyk RW. Aquatic foraging behaviour and freshwater Mussel (*Velesunio* sp.) predation by *Varanus panoptes panoptes* in Central-Western Queensland. International Varanid Intrest Group. 2009; 3(3):85–7.

72. Ciofi C. Varanus komodoensis. In: Pianka ER, King DR, King RA, editors. Varanoid lizards of the world. Bloomington: Indiana University Press; 2004. p. 197–204.

73. R Core Team. R: A language and Environment for Statistical Computing. Vienna: R Foundation for Statistical Computing; 2013.

74. Klingenberg CP, Gidaszewski NA. Testing and quantifying phylogenetic signals and homoplasy in morphometric data. Systematic biology. 2010; 59(3):245–61. doi: 10.1093/sysbio/syp106 PMID: 20525633

75. Wroe S, McHenry C, Thomason J. Bite club: comparative bite force in big biting mammals and the prediction of predatory behaviour in fossil taxa. Proceedings of the Royal Society of London, Series B. 2005; 272:619–25.

76. Pianka E. Lanthanotus borneensis. In: Pianka ER, King DR, King RA, editors. Varanoid Lizards of the World. Bloomington Indiana University Press; 2004. p. 535–8.

77. Wroe S, Ferrara TL, McHenry CR, Curnoe D, Chamoli U. The craniomandibular mechanics of being human. Proceedings of the Royal Society B: Biological Sciences. 2010; 277(1700):3579–86. doi: 10.1098/rspb.2010.0509 PMID: 20554545

78. Figueirido B, Soibelzon LH. Inferring palaeoecology in extinct tremarctine bears (Carnivora, Ursidae) using geometric morphometrics. Lethaia. 2010; 43(2):209–22.

79. Henderson DM. The eyes have it: the sizes, shapes, and orientations of theropod orbits as indicators of skull strength and bite force. Journal of Vertebrate Paleontology. 2003; 22(4):766–78.

80. Fry BG, Wroe S, Teeuwisse W, van Osch MJP, Moreno K, Ingle J, et al. A central role for venom in predation by *Varanus komodoensis* (Komodo Dragon) and the extinct giant *Varanus* (Megalania) *priscus*. Proceedings of the National Academy of Sciences. 2009; 106(22):8969–74. doi: 10.1073/pnas.0810883106

81. Bull J, Jessop TS, Whiteley M. Deathly drool: evolutionary and ecological basis of septic bacteria in Komodo dragon mouths. PLOS one. 2010; 5(6):e11097. doi: 10.1371/journal.pone.0011097 PMID: 20574514

82. Imansyah M, Jessop T, Ciofi C, Akbar Z. Ontogenetic differences in the spatial ecology of immature Komodo dragons. Journal of Zoology. 2008; 274(2):107–15.

83. Rieppel O, Labhardt L. Mandibular mechanics in Varanus niloticus (Reptilia: Lacertilia). Herpetologica. 1979:158–63.

84. Moazen M, Curtis N, O'Higgins P, Jones ME, Evans SE, Fagan MJ. Assessment of the role of sutures in a lizard skull: a computer modelling study. Proceedings of the Royal Society B: Biological Sciences. 2009; 276(1654):39–46. doi: 10.1098/rspb.2008.0863 PMID: 18765341

85. Wang Q, Smith AL, Strait DS, Wright BW, Richmond BG, Grosse IR, et al. The Global Impact of Sutures Assessed in a Finite Element Model of a Macaque Cranium. The Anatomical Record: Advances in Integrative Anatomy and Evolutionary Biology. 2010; 293(9):1477–91. doi: 10.1002/ar.21203

86. Jasinoski SC, Rayfield EJ, Chinsamy A. Functional implications of dicynodont cranial suture morphology. Journal of Morphology. 2010; 271(6):705–28. doi: 10.1002/jmor.10828 PMID: 20077504

87. Reed DA, Porro LB, Iriarte-Diaz J, Lemberg JB, Holliday CM, Anapol F, et al. The impact of bone and suture material properties on mandibular function in *Alligator mississippiensis*: testing theoretical phenotypes with finite element analysis. Journal of Anatomy. 2011; 218(1):59–74. doi: 10.1111/j.1469-7580.2010.01319.x PMID: 21091693

88. Herrel A, Schaerlaeken V, Meyers JJ, Metzger KA, Ross CF. The evolution of cranial design and performance in squamates: Consequences of skull-bone reduction on feeding behavior. 2007. p. 107–17.